

# Deep reinforcement learning control of cylinder flow using rotary oscillations at low Reynolds number

## Introduction

We apply deep neural networks to propose new control strategies considering a classical problem – flow over a cylinder. The optimal control strategy relies on the Reinforcement learning approach and a Policy gradient algorithm with a maximization of a defined reward function. The governing flow control parameter is the rotation velocity of the cylinder around its axis. Experimenting with the angular velocity, the neural network is able to devise a control strategy based on low frequency harmonic oscillations with some additional modulations to stabilize the Kármán vortex street at a low Reynolds number  $Re = 100$ . We examine the convergence issue for two reward functions showing that later epoch number does not always guarantee a better result. The performance of the controller provide the drag reduction of 14% or 16% depending on the employed reward function.

A well-known Kármán vortex street is typically formed in the wake of the flow over a bluff body exerting an oscillating value of the force [1]. This unsteadiness may cause structural damages due to the coupling of the body vibrations and pressure fluctuations of the fluid.

## Problem formulation and computational details

We consider a cylinder of the diameter  $D$  in a fluid cross-flow with a uniform incoming velocity  $U_\infty$  (see Figure 1). The considered Reynolds number  $Re = U_\infty D / \nu = 100$  representing a laminar flow regime with a Kármán vortex shedding, where  $\nu$  is the kinematic viscosity. The applied control strategy is based on the rotation of the cylinder around its axis with the wall velocity:  $U_w(t) = U_\infty \Omega(t)$

The direct numerical simulations (DNS) of the Navier–Stokes equations are employed. The primary goal is to find the optimal signal  $\Omega(t)$  to influence drag and lift coefficients:

$$C_D = \frac{2F_x}{\rho U_\infty^2}, C_L = \frac{2F_y}{\rho U_\infty^2}$$

$$\frac{\partial u_i}{\partial t} + u_j \frac{\partial u_i}{\partial x_j} = -\frac{\partial p}{\partial x_i} + \frac{1}{Re} \frac{\partial^2 u_i}{\partial x_j^2}, \frac{\partial u_j}{\partial x_j} = 0$$

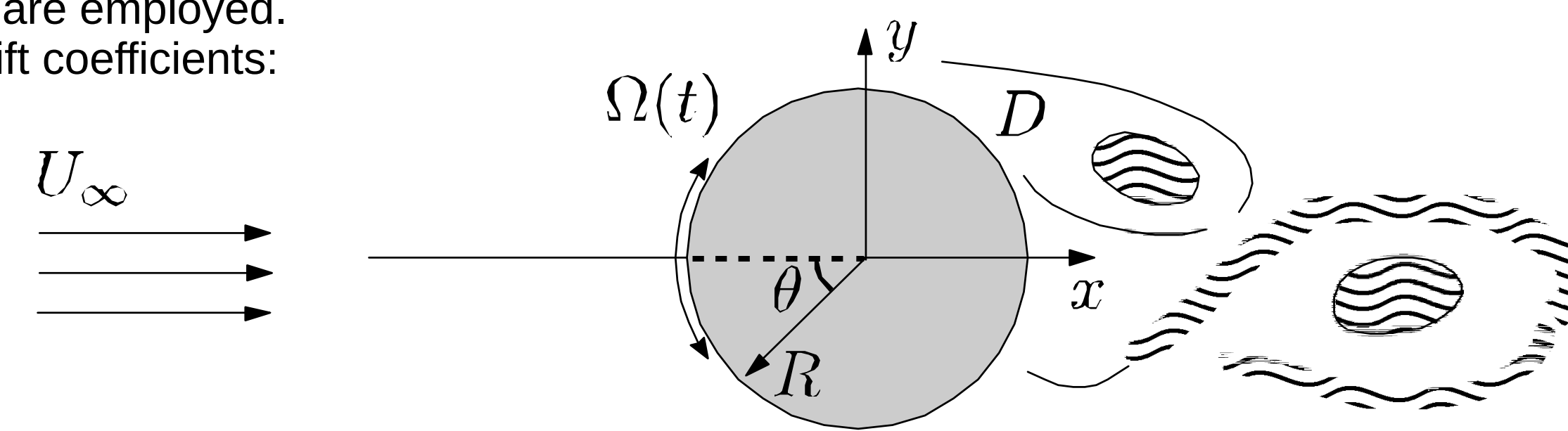


Figure 1. A rotary oscillating cylinder in a cross-flow.

The mesh contains 15,140 hexahedral cells and the computational timestep is  $\Delta t_{CFD} = 10^{-2}$ . The typical quantities of interest are the time-averaged drag coefficient  $C_D = 1.33$  and vortex shedding frequency  $f_{vs} = 0.17$ . The computations are performed using an open source unstructured finite-volume code T-Flows below referred to as the CFD solver [2, 3].

The coupling of the control algorithm and CFD environment is as follows:

- CFD solver obtains current velocity of the cylinder every control time step  $T_{ac} = 30\Delta t_{CFD}$ .
- Computational domain contains an array of  $4 \times 3$  virtual pressure probes behind the cylinder that supply information on the state of the system to the input of the controller's fully-connected neural network (see Figure 2).
- Additionally an optimization algorithm based on Proximal Policy Optimization algorithm from OpenAI Baselines stack obtains reward values for each step which are used during training.

$$r = R_1 - (\langle C_D \rangle_{ac} + R_2 |\langle C_D \rangle_{ac}|),$$

where  $R_1 = 3$ ,  $R_2 = 0.1$  (Case 1 or c1) and 0.2 (Case 2 or c2) [4].

## Results and discussion

Control time step was chosen as  $\sim 10\%$  of the characteristic time scale  $T_{vs} = 1/f_{vs}$  of the vortex shedding (see Figure 3). In order to speedup the training process we employed multi-environment scheme. Below in Figures 4-7 obtained results are presented [5].

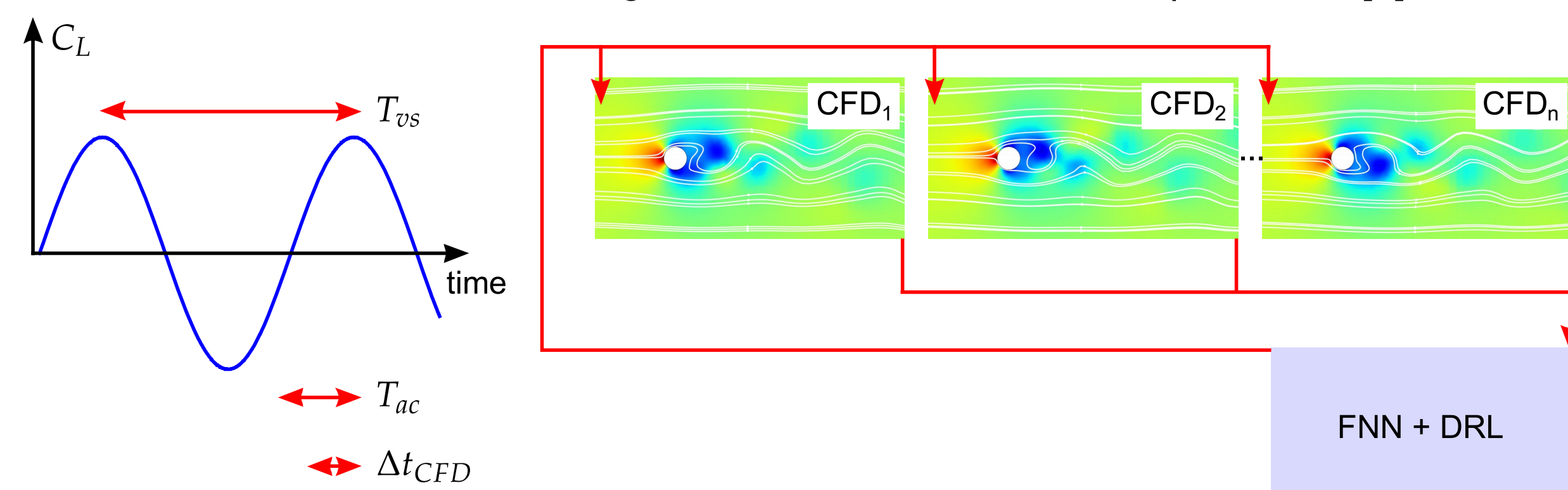


Figure 3. (Left) Illustration of different time scales referred to in the text with the vortex shedding period  $T_{vs}$ , action time step  $T_{ac}$  and CFD time step  $\Delta t_{CFD}$ ; and (Right) multi-environment scheme of the flow control approach.

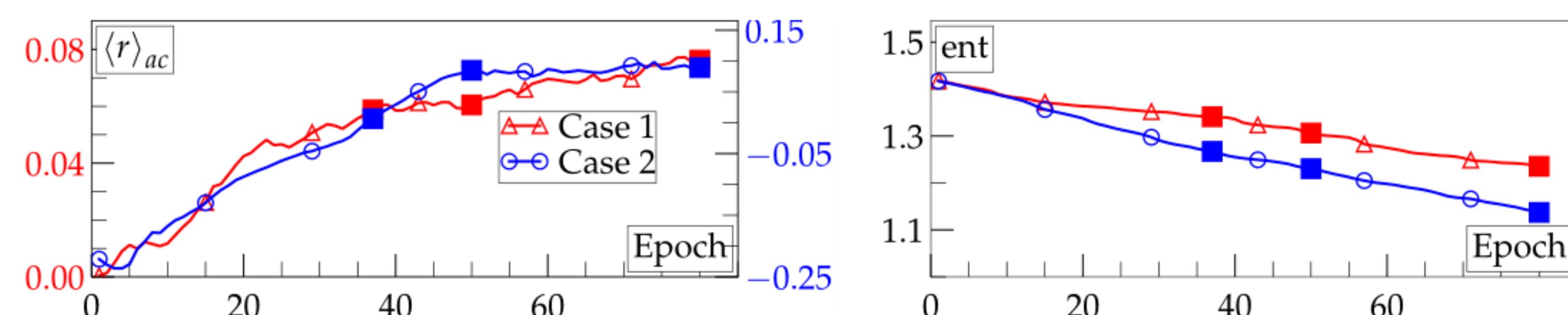


Figure 4. (Left) Evolution of the reward value averaged over the action time step during training (random policy); and (Right) random policy entropy decrease during the optimization process. Square points on both sets correspond to Epochs 37, 50 and 80.

Table 1. Characteristics of several flow regimes corresponding to the number of epoch during the training process, as depicted in Figure 4 by square points.

	c1e37	c1e50	c1e80	c2e37	c2e50	c2e80
$\Delta \bar{C}_D$ (%)	8.1	11.3	13.9	16.1	13.7	14.7
$\Delta(\text{rms } C_L)$ (%)	-50.5	-21.8	29.6	92.8	86.1	76.8
$\Delta \Omega/2$	0.158	0.139	0.082	0.008	0.031	0.126
$\alpha$ (°)	-17.1	1.37	1.39	0.178	2.58	-20.6

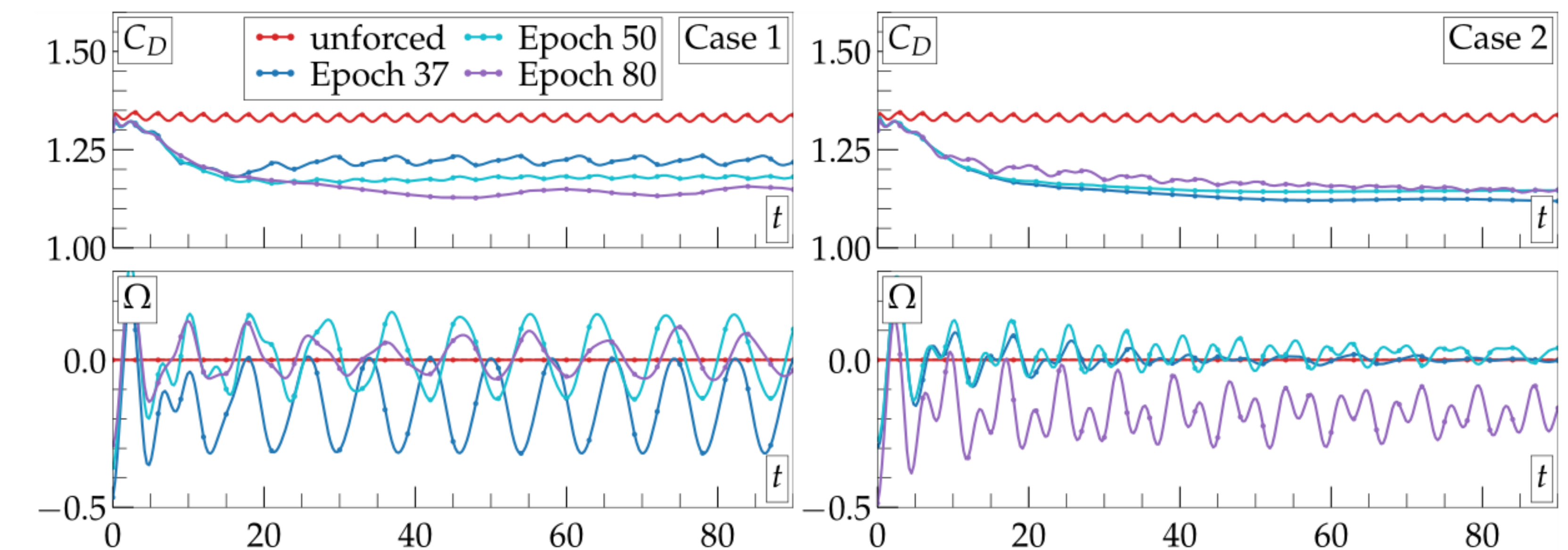


Figure 5. Evolution of  $C_D$  and  $\Omega$  for Cases 1 (Left) and 2 (Right) for different epoch number DRL-based control schemes in comparison with the stationary cylinder flow.

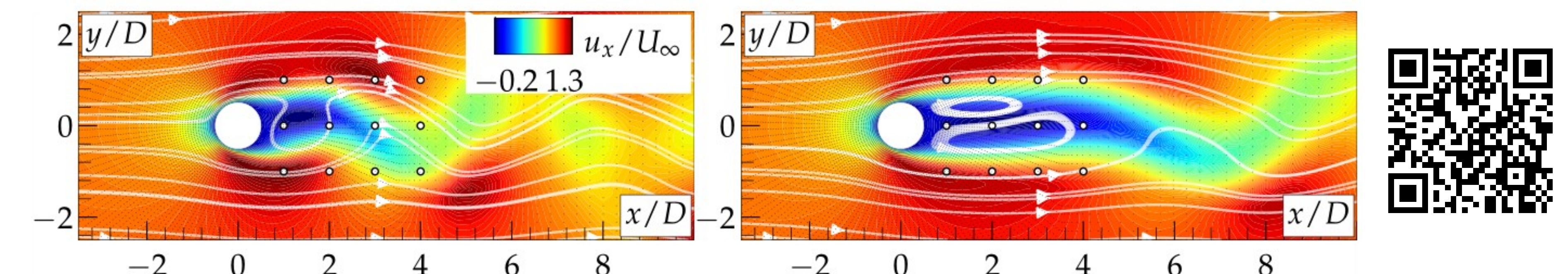


Figure 6. Typical instantaneous streamwise velocity field with streamlines: (Left) stationary cylinder; (Center) DRL-based control for c1e80 after sufficiently long time interval to establish a steady regime. A link (Right) to the movie: <https://youtu.be/9X8XtHk0R84>

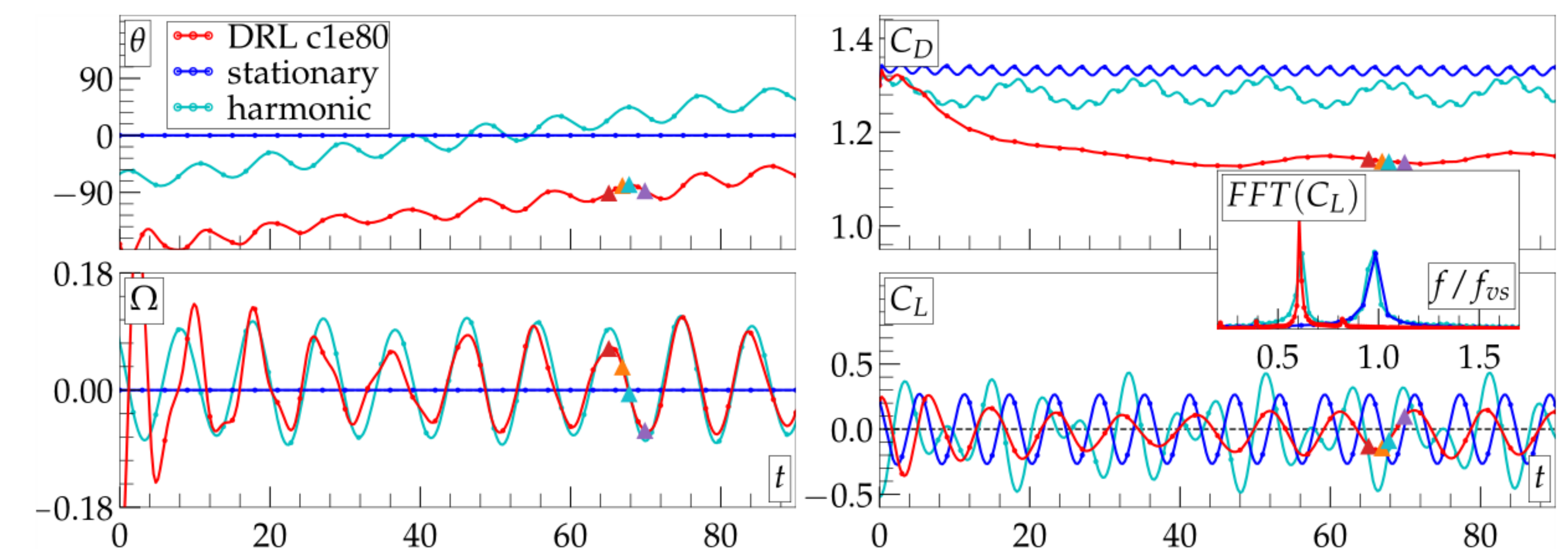


Figure 7. Rotation angle and angular velocity (Left); and the drag and lift coefficients (Right). Three flow regimes are shown: the stationary cylinder (blue line), with a DRL-scheme corresponding to c1e80 for control (red line) and forced with harmonic-based oscillations (cyan line).

## Conclusions

Probing different values of the angular velocity, the neural network was able to create a control strategy based on low frequency harmonic oscillations with some additional modulations to stabilize the Kármán vortex street at a low Reynolds number  $Re = 100$ . The performance of the controller provide the drag reduction of 14% or 16% depending on the employed reward function comparable with a state-of-the-art control theory optimization routines based on adjoint methods.

## References

- 1) Williamson, C. Vortex dynamics in the cylinder wake. *Annu. Rev. Fluid Mech.* 1996, 28, 477–539
- 2) Niceno, B.; Hanjalic, K. Unstructured large eddy and conjugate heat transfer simulations of wall-bounded flows. *Model. Simul. Turbul. Heat Transf.* 2005, 32–73.
- 3) Niceno, B.; Palkin, E.; Mullyadzhyanov, R.; Hadziabdic, M.; Hanjalic, K. T-Flows Web Page. 2018. Available online: <https://github.com/DelNov/T-Flows>
- 4) Rabault, J.; Kuchta, M.; Jensen, A.; Reglade, U.; Cerardi, N. Artificial neural networks trained through deep reinforcement learning discover control strategies for active flow control. *J. Fluid Mech.* 2019, 865, 281–302.
- 5) Tokarev, M.; Palkin, E.; Mullyadzhyanov, R. (2020). Deep Reinforcement Learning Control of Cylinder Flow Using Rotary Oscillations at Low Reynolds Number. *Energies*, 13(22), 5920. (The control code is available online: <https://github.com/AICenterNSU/cylindercontrol>)